ChemPubSoc Europe

DOI: 10.1002/cplu.201600355

CHEMPLUSCHEM Communications

Tuning Gold Nanoparticle Aggregation through the Inhibition of Acid Phosphatase Bioactivity: A Plasmonic Sensor for Light-Up Visual Detection of Arsenate (As^V)

Jia Zhang,*[a] Chuan-Ling Zhang,[b] and Shu-Hong Yu*[a]

Dedicated to Professor Xiurong Yang on the occasion of her 70th birthday.

A plasmonic biosensor for arsenate has been developed which uses gold nanoparticles (AuNPs) as the signal reporter and in which the biocatalytic activity of acid phosphatase (AcP) is modified by the target ion. The enzyme catalyzes the hydrolysis of negatively charged adenosine 5′-monophosphate (AMP) to neutral adenosine, causing appreciable aggregation of AuNPs and then visible color change of the solution from red to blue. The presence of arsenate (As^V), as a molecular analogue of phosphate, can effectively interfere with the bioactivity of AcP by competitive inhibition, and so the hydrolysis process is slowed down. This is reflected by the change in the solution color from blue to red with increasing concentrations of As^V. In contrast to AuNP-based sensors for arsenic (basically As^{III}) that employ the strong interaction between As^{III}-specific molecules and As^{III}, this sensor adopts a different sensing principle and is the first visible sensor for specifically As^V specifically using AuNPs. Finally the practical assay of As^V in groundwater and lake water was performed with satisfactory results, suggesting this approach can be used for quantification of As^V levels in real water samples.

In many areas of the world, groundwater rich in arsenic is used daily for drinking water and irrigation.[1–3] Arsenic usually occurs in the form of inorganic or organic compounds in water, depending upon the specific geological or ecological environment. For example, in reducing aquifers, arsenite (As^{III}) is the dominant form, while arsenate (As^V) is generally the stable form in high-pH aquifers.[4,5] Chronic exposure to arsenic in groundwater can pose significant health issues including skin pigmentation, cardiovascular diseases, and certain cancers.[6,7] The International Agency for Research on Cancer (IARC) and the U.S. Environmental Protection Agency (EPA) have classified arsenic as a human carcinogen for many years.[8] Toxicity studies show that inorganic arsenic species are much more harmful than their organic counterparts (readily released by the body),[9] and this awareness of toxicity is conductive to arsenic speciation rather than total arsenic determination.[10]

For decades, the development of sensors for arsenic anions has made substantial advances in terms of sensitivity and selectivity. Electrochemical assays based on the surface modification of electrodes is one of the most effective methods to achieve low detection limits,[11–13] which are comparable to or below the maximum value for arsenic (10 ppb, 0.13 μM) in drinking water determined by the World Health Organization (WHO). Another approach features the use of visual methods,[14–16] that is, colorimetry and fluorometry, which are favorable for rapid field testing of the arsenic level in those identified and predicted arsenic-affected regions and areas. A frequently used strategy to detect inorganic arsenic visually is first to form arsine by hydride generation and followed by colorimetric determination with molybdenum blue,[17] but this method is extremely dangerous due to the highly toxic arsine gas. Recently, AuNP-based colorimetry has emerged as an interesting strategy for the detection of arsenic anions.[18–24] This approach is based on the color/optical change of a AuNP solution dictated by the interparticle distance[25] at different concentrations of arsenic. The recognition elements for arsenic are thiol molecules,[18,21,23] ionic liquids,[24] and oligonucleotides,[19,20,22] with As^{III} being targeted, yet in natural waters, As^V is typically predominant.[10] Therefore, it is desirable to fabricate colorimetric nanosensors for As^V to complement those designed for As^{III}.

Herein, we present a method for the light-up colorimetric detection of arsenate by means of the arsenate-controlled bioactivity of acid phosphatase (AcP) which affects the interparticle distance of AuNPs. The detection is based on the inhibitory effect of arsenate on AcP bioactivity[26] for the hydrolysis of the charged nucleotide to the uncharged nucleoside, with citrate-capped AuNPs as the optical probe. To be more specific, the principle of detection is outlined in Scheme 1. We chose adenosine 5′-monophosphate (AMP) to be the substrate for AcP. Since the enzymatic reaction is optimal under weakly acidic conditions while the colorimetric response is preferable under alkaline conditions, we divided the detection procedure into two separate steps. In acetate buffer (buffer I, 10 mM, pH 5.0, containing 10 mM $MgCl_2$ to activate the enzyme) AcP initially

[a] Dr. J. Zhang, Prof. Dr. S.-H. Yu
Division of Nanomaterials and Chemistry
Hefei National Laboratory for Physical Sciences at the Microscale
Collaborative Innovation Center of Suzhou Nano Science and Technology
Department of Chemistry, Hefei Science Center of CAS
University of Science and Technology of China
Hefei, Anhui 230026 (China)
E-mail: shyu@ustc.edu.cn

[b] Dr. C.-L. Zhang
School of Chemistry and Chemical Engineering
Hefei University of Technology
Hefei, Anhui 230029 (China)

Supporting information for this article can be found under http://dx.doi.org/10.1002/cplu.201600355.

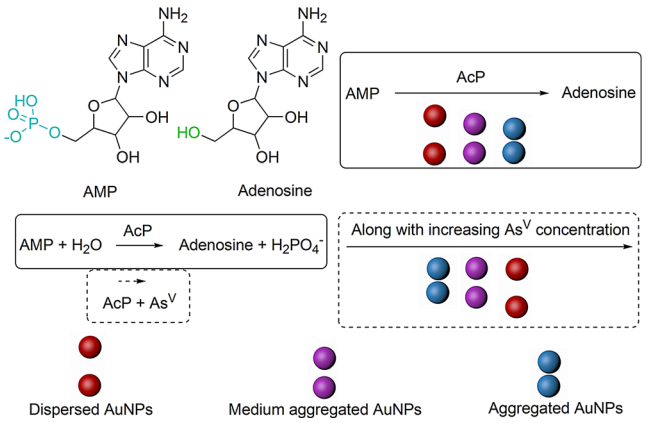

Scheme 1. Principle of the detection of As^V. Owing to the catalysis of AcP, the charged AMP is converted to uncharged adenosine, and when bare AuNPs are introduced into the solution, the interparticle distance becomes closer; thus the color of the solution turns from red through purple to blue, depending on the progress of the enzymatic reaction. In the presence of As^V, the catalytic hydrolysis is retarded due to the inhibition of AcP activity, and the color of solution reverses from blue through purple back to red, depending on the concentration of As^V.

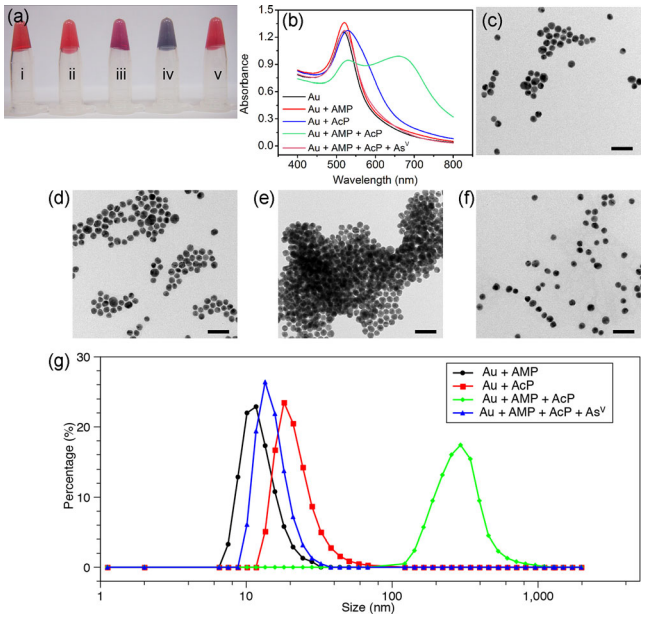

Figure 1. a) Color of AuNP solution alone (i) and in the presence of AMP (ii), AcP (iii), AMP+AcP after enzymatic reaction (iv), and AMP+AcP after enzymatic reaction in the presence of As^V (v). b) Optical spectra corresponding to the solutions in (a). c–f) Representative TEM images of AuNPs in the presence of AMP (c), AcP (d), AMP+AcP after enzymatic reaction (e), and AMP+AcP after enzymatic reaction in the presence of As^V (f). Scale bars: 50 nm. g) DLS profile showing the HDs of AuNPs under different conditions. AMP: 0.3 mM, AcP: 0.29 μM, As^V: 0.1 mM, and AuNPs: 4.7 nM.

catalyzes the dephosphorylation of AMP to adenosine. In phosphate buffer (buffer II, 50 mM, pH 9.0) AMP protects AuNPs from aggregation in solution owing to the charge from the phosphate group, but adenosine causes the AuNPs to aggregate since the nucleoside can displace weakly bound citrate ions and bind to AuNPs via metal–ligand interactions.[27] As a result, a change in the color of the solution from red through purple to blue can be observed with the gradual generation of adenosine. As^V, a molecular analogue of phosphate, can compete with AMP in the enzymatic reaction and acts as an inhibitor on the AcP activity. As a result, the change in the color of the solution is reversed and observed from blue through purple to red when the concentration of As^V increases gradually.

To test the scheme, we studied the effect of 0.1 mM of As^V. First we added 2 μL of AcP solution (1.2 unit/mL, or 2.9 μM),[28] 2 μL of As^V solution (1 mM), and 6 μL of AMP solution (1 mM) to 10 μL of buffer I and incubated the resulting solution at 37 °C for 80 min. Then we transferred 10 μL of the above solution into the probe solution (200 μL, 7.0 nM AuNPs + 100 μL buffer II), mixed for 10 s, and recorded the spectra after 5 min. As shown in Figure 1 a, after the enzymatic hydrolysis has taken place, the color of the AuNP solution in the absence of As^V is blue (iv), in stark contrast to the color of the untreated AuNP solution (i) and AuNP solution incubated with AMP only (ii). The optical spectrum of the blue solution shows the strong damping of surface plasmon band (SPB) at 520 nm and the appearance of a second SPB at 660 nm (Figure 1 b, green line) owing to the interparticle plasmon coupling of AuNPs.[29–31] This spectrum is similar to that of the solution incubated with adenosine (Figure S1, Supporting Information), indicating the catalytic conversion of AMP to adenosine. However, in the presence of As^V, the color of the solution returns to red (Figure 1 a, (v)) with the disappearance of the second SPB (Figure 1 b, pink line), indicating the stabilization of AuNPs by AMP due to the inhibition of AcP bioactivity by arsenate. The degrees of particle aggregation are also supported by transmission electron microscopy (TEM) (Figure 1 c, (e, f)). To avoid the effects of sample drying in a particular state, we characterized the hydrodiameters (HDs) of AuNPs under specific conditions by dynamic light scattering (DLS). As shown in Figure 1 g, the DLS result is quite consistent with the other results. It should be noted that some degree of particle aggregation is observed for only AcP, as shown in Figure 1 a (iii), b (blue line), and d. This suggests that the aggregation of AuNPs comes from the synergistic effects of adenosine and AcP, yet the effect of adenosine is much more appreciable than that of AcP.

A few parameters relevant to the aggregation of nanoparticles need to be optimized. Apart from AMP, we also studied the kinetic enzymatic hydrolysis of adenosine 5′-diphosphate (ADP) and adenosine 5′-triphosphate (ATP), and the results are shown in Figure S2 a in the Supporting Information. The ratio of the absorbances at 660 and 520 nm (A_{660}/A_{520}) was chosen to assess the degree of aggregation and also as a measure of the color change from red to blue. The same concentrations of the three nucleotides were chosen in order to normalize the concentration of adenosine. Besides, the amounts of AcP are also identical. We find that higher absorbance ratios are obtained in the ascending order of ATP, ADP, and AMP. Significant aggregation of nanoparticles occurs only after 80 min of enzymatic reaction in the case of AMP, while no marked aggregation can be seen for ATP within the overall test time. We ascribe the phenomena to the slow rates of hydrolysis and the multistep dephosphorylation od ADP and ATP.[32] Because the

absorbance ratio is a combined result from adenosine and AcP, we did not estimate the progress of the enzymatic conversion of AMP. We then optimized the concentration of AMP (Figure S2b). We found that A_{660}/A_{520} is nearly in proportion to the concentration of AMP. The largest slope of variation is obtained at 0.225 mM of AMP, followed by that at 0.3 mM of AMP. However, the absorbance ratios for both concentrations of AMP almost reach the same in the end. We conducted the experiment with 0.3 mM of AMP and then optimized the amount of AcP, as shown in Figure S2c. Clearly, the more AcP is used, the higher the rate of hydrolysis, yet the slope of variation at 0.29 μM of AcP is similar to that at 0.44 μM of AcP. Therefore, we chose 0.29 μM as the optimum amount of AcP. Based on the knowledge that the detection of arsenate is virtually a process of dispersion of nanoparticles, it is better to select a time for hydrolysis reaction sharing the highest sensitivity relative to particle aggregation. Results shown in Figure S2d support our hypothesis. When the concentration of AMP is 0.3 mM, the best response to arsenate is obtained at 80 min of enzymatic reaction, when the color change of the solution from red to blue reaches its optimum sensitivity, as shown in Figure S2b. Moreover, selecting 80 min for the enzymatic reaction, we do not observe a meaningful difference in the response to arsenate by use of 0.225 mM of AMP compared to that using 0.3 mM of AMP. Taken together, the conditions for the sensing of As^V were selected to be 0.3 mM of AMP, 0.29 μM of AcP, and 80 min of enzymatic hydrolysis. In addition, even though the adenosine-induced AuNP aggregation is rapid, for better reproducibility, the time for the colorimetric response was set to be 5 min.

We applied the optimal conditions described above for the sensing of As^V. The gradual damping of the second SPB along with the increase of As^V concentration (Figure 2a) indicates that interference by As^V with the enzymatic hydrolysis of AMP is in effect. An exponential decay curve is obtained ($y = 0.13 + 0.80\exp(-x/3.97)$, $0.1 \le x \le 100$) between the absorbance ratio A_{660}/A_{520} and As^V concentration (Figure 2b); specifically, a linear relationship is established up to 1.0 μM, with a sensitivity of $0.33 \pm 0.04\ \mu M^{-1}$ and a detection limit of ca. 0.1 μM at a signal-to-noise ratio of 3 (Figure 2b, inset). Corresponding to the spectral profile, the color change of the solution from blue (0, 0.1, and 0.5 μM) through purple (1 and 5 μM) to red (above 10 μM) can be clearly seen with the naked eye (Figure 2c). The limit of visual discrimination is about 0.5 μM. Since this is the first AuNP-based plasmonic sensor for As^V only, comparison of the visual detection limits among different sensors cannot be done. On the other hand, compared to plasmonic nanosensors for As^{III},[18–24] the present one may not be advantageous in the spectral limit of detection but shows comparable visual detection limit. Although this visible limit of detection is somewhat higher than the maximum arsenic level in drinking water set by the WHO, our method may find prospective application in arsenic testing, owing to its simplicity, at fields where relatively high concentrations of As^V are expected.

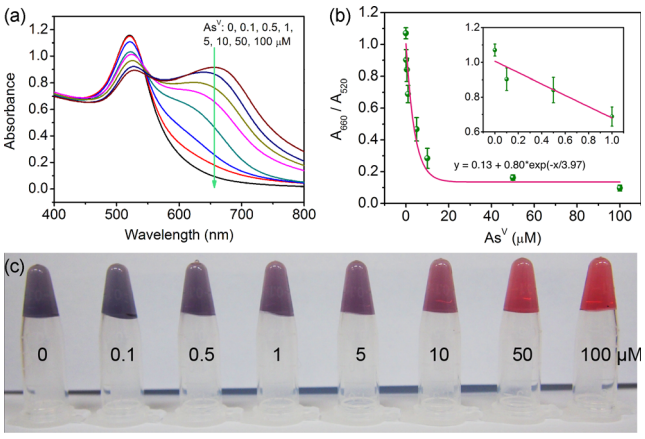

Figure 2. The sensing performance of the sensor operated in deionized water. a) Variation of optical spectra in the presence of different concentrations of As^V. b) Calibration curves for absorbance ratio (A_{660}/A_{520}) versus the concentration of As^V. The error bars show standard deviations that are based on three measurements. c) Colorimetric response of AuNP solution in the presence of different concentrations of As^V. Conditions: 0.3 mM of AMP, 0.29 μM of AcP, 80 min for enzymatic hydrolysis, and 5 min for colorimetric response.

To investigate the sensor selectivity, many ions commonly encountered in groundwater and surface water were examined. We found that most of the ions including As^{III} induce no reverse effects on the colorimetric response, with the exception of Cu^{2+}, F^-, and $H_2PO_4^-$ ions (Figure S3). These three ions exert pronounced effects on the dispersion of nanoparticles through the inhibition of AcP activity, as previously identified.[32] The three ions do not interfer when their concentrations are less than 1 μM for Cu^{2+}, 10 μM for F^-, and 1 μM for $H_2PO_4^-$. Meanwhile, there are no obvious interferences in the detection of As^V in solutions incubated with the other ions under specific conditions. Of the three ions, phosphate may present the biggest problem since it can coexist with As^V in groundwater. Therefore, for water samples with potentially high phosphate levels, this approach is not useful unless there are viable ways to remove phosphate without influence on As^V.

Groundwater from the local countryside was spiked with As^V and used as a model of arsenic-contaminated drinking water. Both the spectral change and the solution color change (Figure 3a, b) resemble with those observed for the calibration of As^V in deionized water (Figure 2a, c). Indeed, we observe little difference between their working curves; the two absorbance ratios at a given concentration are very close (Figure 3c). We further tested the recovery after adding known concentrations of As^V to a campus lake water sample. The results show that the recovery is in the range of 95% to 105% (Figure S4). Apart from the detection of As^V, the system can also be used to detect As^{III} through the oxidation of As^{III} to As^V by hypochlorite and the removal of residual hypochlorite by the addition of sulfite (data not shown). Even though more real water samples, including contaminated ones, have to be tested for validation of this method, the data discussed above indicate that the sensor has the capacity to detect As^V in water samples with sufficient selectivity and sensitivity.

In summary, we have developed the first light-up plasmonic nanosensor for As^V through As^V-controlled AcP bioactivity and gold nanoparticle aggregation. Unlike assays for As^{III} using

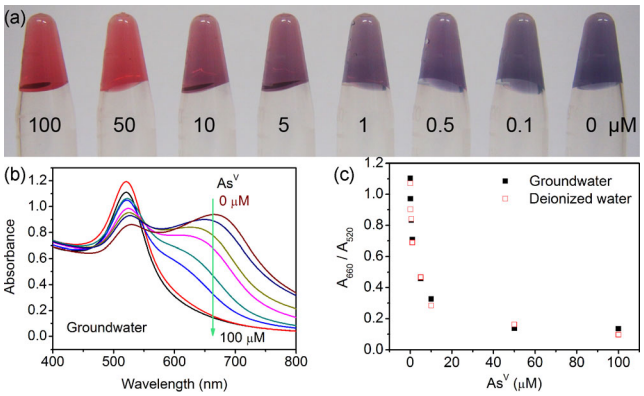

Figure 3. The sensing performance of the sensor operated in groundwater spiked with known amounts of As^V. a) Colorimetric response of AuNP solution in the presence of different concentrations of As^V. b) Variation of optical spectra in the presence of different concentrations of As^V. c) Performance comparing the assay in deionized water with the assay in groundwater. The data are based on the average of three measurements, with error bars removed for clarity. Conditions: 0.3 mM of AMP, 0.29 μM of AcP, 80 min for enzymatic hydrolysis, and 5 min for colorimetric response.

gold nanoparticles and As^{III}-specific molecules in literature, this detection is founded on the inhibitory effect of As^V on AcP in the enzymatic dephosphorylation of AMP, leading to the dispersion of nanoparticles and visible change in the color of the solution from blue to red. The sensor is endowed with quite remarkable selectivity towards As^V even in the presence of most of environmentally relevant ions, and relatively low detection limit meeting with the requirement of visible assaya of arsenic-enriched waters. As a plasmonic nanosensor for As^V, our method makes good complement to those designed for As^{III}. Our next step is to decrease the visible discrimination limit below the standard of the WHO. A novel practice using enzyme-guided crystal growth with inverse sensitivity[33] might be a good measure of solution, which is currently under investigation.

Experimental Section

Materials

Acid phosphatase (EC 3.1.3.2) from potato (solid, 3–10 units/mg) was purchased from Sigma–Aldrich. Sodium hydrogenarsenate heptahydrate (As^V) was purchased from Xiya Reagent (Chengdu, China). Nucleotides were purchased from Sangon Biotech (Shanghai, China). Other chemicals were analytical grade and used without further purification. Deionized water was used throughout the experiments.

Citrate-capped gold nanoparticles of 13 nm average diameter were synthesized according to the literature.[34] The particle concentration was calculated to be 7.0 nM, based on extinction coefficient of $2.7\times10^8\ M^{-1}\,cm^{-1}$.[35]

The detection of As^V in deionized water was conducted in two separate steps. First, 10 μL of acetate buffer (10 mM, pH 5.0, containing 10 mM $MgCl_2$) was treated with 2 μL of AcP (1.2 unit/mL), 2 μL of varied concentrations of As^V, and 6 μL of AMP (1 mM), and the solution was incubated at 37 °C for 80 min. Second, 300 μL of solution containing 200 μL of gold suspension and 100 μL of phosphate buffer (50 mM, pH 9.0) was treated with 10 μL of the above solution from the first step; the resulting solution was mixed for about 10 s, and the spectrum was recorded after 5 min of incubation.

The assay of As^V in practical water samples was conducted by following the above procedure, except that groundwater and lake water were used instead of deionized water. Prior to testing, groundwater and lake water were pretreated with filter membrane (0.22 μm size cut-off) to avoid possible interference from microbes and other substances.

Characterization

UV/Vis optical absorption spectra were obtained on a Lambda 25 UV/Vis spectrometer (PerkinElmer). Transmission electron microscopy images of the nanoparticles were acquired on a JEOL-2100F transmission electron microscope (JEOL) operating at 200 kV. DLS measurements were performed on a Malvern Zetasizer instrument.

Acknowledgements

We acknowledge support from the National Basic Research Program of China (grants 2014CB931800, 2013CB931800), the National Natural Science Foundation of China (grants 21407140, 21431006), and the Chinese Academy of Sciences (grant KJZD-EW-M01–1). J.Z. thanks the Research Funds for the Central Universities (grant WK2060190036).

Keywords: acid phosphatase · arsenate · gold nanoparticles · sensors · water

[1] M. Amini, K. C. Abbaspour, M. Berg, L. Winkel, S. J. Hug, E. Hoehn, H. Yang, C. A. Johnson, *Environ. Sci. Technol.* **2008**, *42*, 3669.
[2] L. Winkel, M. Berg, M. Amini, S. J. Hug, C. A. Johnson, *Nat. Geosci.* **2008**, *1*, 536.
[3] L. Rodriguez-Lado, G. F. Sun, M. Berg, Q. Zhang, H. B. Xue, Q. M. Zheng, C. A. Johnson, *Science* **2013**, *341*, 866.
[4] P. L. Smedley, D. G. Kinniburgh, *Appl. Geochem.* **2002**, *17*, 517.
[5] E. M. Muehe, A. Kappler, *Environ. Chem.* **2014**, *11*, 483.
[6] C. Hopenhayn-Rich, M. L. Biggs, A. H. Smith, *Int. J. Epidemiol.* **1998**, *27*, 561.
[7] A. H. Smith, E. O. Lingas, M. Rahman, *Bull. World Health Org.* **2000**, *78*, 1093.
[8] S. W. Shen, X. F. Li, W. R. Cullen, M. Weinfeld, X. C. Le, *Chem. Rev.* **2013**, *113*, 7769.
[9] C. K. Jain, I. Ali, *Water Res.* **2000**, *34*, 4304.
[10] Z. L. Gong, X. F. Lu, M. S. Ma, C. Watt, X. C. Le, *Talanta* **2002**, *58*, 77.
[11] C. Gao, X. Y. Yu, S. Q. Xiong, J. H. Liu, X. J. Huang, *Anal. Chem.* **2013**, *85*, 2673.
[12] D. M. Wang, Y. W. Zhao, H. L. Jin, J. X. Zhuang, W. M. Zhang, S. Wang, J. C. Wang, *ACS Appl. Mater. Interfaces* **2013**, *5*, 5733.
[13] H. H. Chen, J. F. Huang, *Anal. Chem.* **2014**, *86*, 12406.
[14] S. Roy, G. Palui, A. Banerjee, *Nanoscale* **2012**, *4*, 2734.
[15] M. Baglan, S. Atilgan, *Chem. Commun.* **2013**, *49*, 5325.
[16] B. W. Liu, J. W. Liu, *Chem. Commun.* **2014**, *50*, 8568.
[17] K. Toda, T. Ohba, M. Takaki, S. Karthikeyan, S. Hirata, P. K. Dasgupta, *Anal. Chem.* **2005**, *77*, 4765.
[18] J. R. Kalluri, T. Arbneshi, S. A. Khan, A. Neely, P. Candice, B. Varisli, M. Washington, S. McAfee, B. Robinson, S. Banerjee, A. K. Singh, D. Senapati, P. C. Ray, *Angew. Chem. Int. Ed.* **2009**, *48*, 9668; *Angew. Chem.* **2009**, *121*, 9848.
[19] Y. G. Wu, L. Liu, S. S. Zhan, F. Z. Wang, P. Zhou, *Analyst* **2012**, *137*, 4171.

[20] Y. G. Wu, S. S. Zhan, F. Z. Wang, L. He, W. T. Zhi, P. Zhou, *Chem. Commun.* **2012**, *48*, 4459.
[21] N. Xia, Y. F. Shi, R. C. Zhang, F. Zhao, F. Liu, L. Liu, *Anal. Methods* **2012**, *4*, 3937.
[22] R. P. Liang, Z. X. Wang, L. Zhang, J. D. Qiu, *Chem. Eur. J.* **2013**, *19*, 5029.
[23] P. Nath, R. K. Arun, N. Chanda, *RSC Adv.* **2014**, *4*, 59558.
[24] Z. Q. Tan, J. F. Liu, Y. G. Yin, Q. T. Shi, C. Y. Jing, G. B. Jiang, *ACS Appl. Mater. Interfaces* **2014**, *6*, 19833.
[25] K. Saha, S. S. Agasti, C. Kim, X. N. Li, V. M. Rotello, *Chem. Rev.* **2012**, *112*, 2739.
[26] S. Cosnier, C. Mousty, X. Q. Cui, X. R. Yang, S. J. Dong, *Anal. Chem.* **2006**, *78*, 4985.
[27] W. A. Zhao, W. Chiuman, J. C. F. Lam, M. A. Brook, Y. F. Li, *Chem. Commun.* **2007**, 3729.
[28] The AcP concentration was calculated according to the information of the supplier (Sigma–Aldrich, p1146dat.pdf). The specific activity of the enzyme is assumed to be 6 units/mg solid. Since the molecular mass is 69 kDa, then 1 unit corresponds to 2.42 nmol.
[29] J. S. Lee, P. A. Ulmann, M. S. Han, C. A. Mirkin, *Nano Lett.* **2008**, *8*, 529.
[30] X. J. Xie, W. Xu, T. H. Li, X. G. Liu, *Small* **2011**, *7*, 1393.
[31] H. B. Wang, W. Xu, H. Zhang, D. W. Li, Z. Q. Yang, X. J. Xie, T. H. Li, X. G. Liu, *Small* **2011**, *7*, 1987.
[32] Y. Sugiura, H. Kawabe, H. Tanaka, S. Fujimoto, A. Ohara, *J. Biol. Chem.* **1981**, *256*, 664.
[33] L. Rodríguez-Lorenzo, R. de La Rica, R. A. Alvarez-Puebla, L. M. Liz-Marzan, M. M. Stevens, *Nat. Mater.* **2012**, *11*, 604.
[34] K. G. Grabar, R. G. Freeman, M. B. Hommer, M. J. Natan, *Anal. Chem.* **1995**, *67*, 735.
[35] J. Lee, S. I. Stoeva, C. A. Mirkin, *J. Am. Chem. Soc.* **2006**, *128*, 8899.

Manuscript received: July 4, 2016
Accepted Article published: July 19, 2016
Final Article published: ■■ ▮▮, 0000

COMMUNICATIONS

J. Zhang, C.-L. Zhang, S.-H. Yu**

■■ – ■■

Tuning Gold Nanoparticle Aggregation through the Inhibition of Acid Phosphatase Bioactivity: A Plasmonic Sensor for Light-Up Visual Detection of Arsenate (As^V)

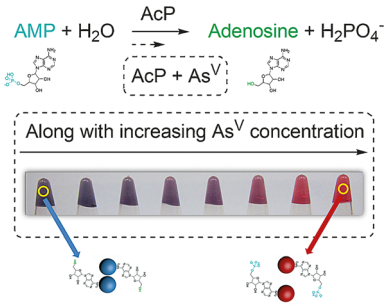

Good As^V gold: The first colorimetric sensor specifically for arsenate makes use of gold nanoparticles. The sensing rationale relies on the selective inhibition of acid phosphatase bioactivity by arsenate, leading to the reversal of solution color from blue to red.